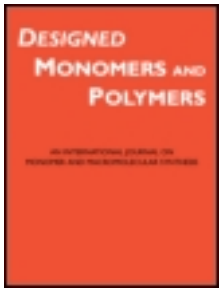

Designed Monomers and Polymers
Publication details, including instructions for authors and subscription information:
http://www.tandfonline.com/loi/tdmp20

Stimuli-responsive nanofibers prepared from poly(N-isopropylacrylamide-acrylamide-vinylpyrrolidone) by electrospinning as an anticancer drug delivery

Roya Salehi [a], Mohammad Irani [b], Mohammad-Reza Rashidi [c], Abdolreza Aroujalian [b], Ahmadreza Raisi [b], Morteza Eskandani [c], Ismaeil Haririan [d e] & Soudabeh Davaran [c]

[a] Drug Applied Research Center, Tabriz University of Medical Sciences, Tabriz, Iran

[b] Department of Chemical Engineering, Amirkabir University of Technology (Tehran Polytechnic), Hafez Ave., P.O. Box 15875-4413, Tehran, Iran

[c] Research Center for Pharmaceutical Nanotechnology, Tabriz University of Medical Sciences, Tabriz, Iran

[d] Department of Pharmaceutics, School of Pharmacy, Tehran University of Medical Sciences, Tehran, Iran

[e] Medical Biomaterials Research Center (MBRC), Tehran University of Medical Science, Tehran, Iran

Version of record first published: 27 Feb 2013.

To cite this article: Roya Salehi , Mohammad Irani , Mohammad-Reza Rashidi , Abdolreza Aroujalian , Ahmadreza Raisi , Morteza Eskandani , Ismaeil Haririan & Soudabeh Davaran (2013): Stimuli-responsive nanofibers prepared from poly(N-isopropylacrylamide-acrylamide-vinylpyrrolidone) by electrospinning as an anticancer drug delivery, Designed Monomers and Polymers, DOI:10.1080/15685551.2013.771303

To link to this article: http://dx.doi.org/10.1080/15685551.2013.771303

Designed Monomers and Polymers, 2013
http://dx.doi.org/10.1080/15685551.2013.771303

Stimuli-responsive nanofibers prepared from poly(N-isopropylacrylamide-acrylamide-vinylpyrrolidone) by electrospinning as an anticancer drug delivery

Roya Salehi[a], Mohammad Irani[b], Mohammad-Reza Rashidi[c], Abdolreza Aroujalian[b], Ahmadreza Raisi[b], Morteza Eskandani[c], Ismaeil Haririan[d,e]* and Soudabeh Davaran[c]*

[a]*Drug Applied Research Center, Tabriz University of Medical Sciences, Tabriz, Iran;* [b]*Department of Chemical Engineering, Amirkabir University of Technology (Tehran Polytechnic), Hafez Ave., P.O. Box 15875-4413, Tehran, Iran;* [c]*Research Center for Pharmaceutical Nanotechnology, Tabriz University of Medical Sciences, Tabriz, Iran;* [d]*Department of Pharmaceutics, School of Pharmacy, Tehran University of Medical Sciences, Tehran, Iran;* [e]*Medical Biomaterials Research Center (MBRC), Tehran University of Medical Science, Tehran, Iran*

(*Received 18 November 2012; final version received 27 January 2013*)

In this study, stimuli-responsive nanofibers (NFs) were successfully prepared via electrospinning method. Poly(N-isopropylacrylamide-*co*-acrylamide-*co*-vinylpyrrolidone) P(NIPAAM-AAm-VP) was used as the material for preparing the electrospinning NFs. Doxorubicin (Dox)-loaded NFs were prepared and characterized by XRD, Scanning electron microscopy and FTIR. A response surface methodology was used to evaluate the effect of key parameters on the fiber diameter. The cytotoxicity of Dox-loaded NFs was evaluated by 3-(4,5-dimethylthiazol-2-yl)-2,5-diphenyltetrazolium bromide, a tetrazole assay on lung cancer A549 cell lines. *In vitro* cytotoxicity assay showed that the P(NIPAAM-AAm-VP) fibers themselves did not affect the growth of A549 cells. Antitumor activity of the Dox-loaded fibers against the cells was kept over the whole experimental process, while that of pristine Dox disappeared within 48 h. Drug release pattern from these systems is in zero order and drug release rate is not dependent on drug/polymer ratio in different implant formulations. These novel NFs were stable and preserved their morphology even after incubation in release medium (pH 7.4, 37 °C), while collapsed and dispersed quickly in aqueous solution of acidic medium at room. The reported incorporation of stimuli-responsive properties into NFs takes advantage of their extremely large surface area and porosity and is expected to provide a simple platform for smart drug delivery.

Keywords: nanofibrous scaffold; Box–Behnken design; electrospinning; cytotoxicity; doxorubicin; sustained release

1. Introduction

The principle of controlled-release drug therapy involves the delivery of a predetermined amount of drug, over a specified period of time, in a predictable behavior. The aim of all controlled-release systems is to develop the effectiveness of drug therapy.[1,2] Recently, there has been a growing attention in the development of novel drug delivery systems (DDSs) to improve the effectiveness of chemotherapy and efficiency of radiotherapy after chemotherapy, to reduce toxic side effects of anticancer drugs, and to achieve stable storage and selective targeting.[3,4] At the heart of these progresses is the electrospinning method, which plays an important role in the production of nanoscale fiber of biomaterials ranging from polymers and ceramics to their composites. Inparticular, many natural and synthetic polymers have been transformed into fibers with diameters in the range of tens to hundreds of nanometers.[5–8] Fibrous scaffolds, such as the system made up by electrospinning [9–12] have been used in several biomedical applications especially as vehicles for controlled drug delivery.[13,14] Application of nanofibrous electrospun scaffolds has many advantages in drug delivery, especially for site-specific and low-dosage forms of infection and anticancer DDSs. The development of smart or stimuli-responsive NFs that have the ability to respond to very slight changes in the environment, such as temperature,[15] pH [16], is critically important for controlling biological responses in biotechnological and biomedical applications, and because of the resulting large and tunable surface area and porosity. Poly(N-isopropylacrylamide) (PNIPAAm) is a smart polymer that has been studied the most extensively. Poly-NIPAAm in an aqueous solution exhibits lower critical solution temperature (LCST) at 32 °C because of hydrogen-bonding interactions between the amide group and water. Hydrogen bonds are bound to the hydrophilic moieties and the polymer is in a swollen conformation below LCST, and in a shrinkage state

*Corresponding authors. Emails: haririan@tums.ac.ir (I. Haririan); davaran@tbzmed.ac.ir (S. Davaran).

while the temperature is higher than LCST. Electrospun NFs of NIPAAm homopolymer are not stable in water and disperse easily; therefore, copolymerization with desired co-monomers is required to obtain stable NFs in an aqueous medium. On the other hand, electrospinning of water-soluble polymers contributes to the dissolution of the resulting high hydrophilic fibers, which limits its application in some areas, especially in biomedical engineering. The crosslinking of hydrophilic polymers is a good way to prepare less water-soluble or water-insoluble fibers. The crosslinking reactions have been performed by chelation crosslinking, thermal curing, oxidative crosslinking, or radiation crosslinking (e.g. X-ray, UV, etc.) [15,17] or physical crosslinking. Physical crosslinking can be accomplished by ionic or hydrophobic interactions.[18] Physical crosslinking is preferable because of its nonpolluting advantages.

Solubility and compatibility of the drugs in the drug/polymer/solvent system were the decisive factors for the preparation of electrospun fiber formulation. In most cases, electrospinning was performed in general organic solvents.[19–21] For many applications, such as tissue engineering, biomedical, agricultural, etc. the toxicity of the organic solvent used could be highly critical. However, organic solvents are toxic, so that it is preferable to use nontoxic aqueous systems for potential biomedical applications. The diameter of NFs prepared by electrospinning can be controlled by various parameters such as polymer solution properties, process and ambient conditions.[22–24] Solution parameters such as viscosity, conductivity, and surface tension; process parameters such as voltage, distance between needle tip and the collector, and geometry of collector; and ambient parameters such as temperature and humidity affects the formation of the fibers and fiber morphologies. Investigation of each factor separately would be very time consuming and if several factors play a role, their interactions would not be discernable even if they were dominated. Therefore, statistical experimental design methods can be used to evaluate the effects of variables and optimization of experimental parameters. Response surface methodology (RSM) is essentially a particular set of mathematical and statistical methods for experimental design and evaluating the effects of variables and searching optimum conditions of variables.[25] In recent researches, the factor space central composite design (CCD) and Box–Behnken design (BBD) are commonly selected experimental design techniques.[25,26] However, for a quadratic response surface model with three or more factors, the BBD technique is much more advantageous when compared to CCD.[25,27]

Doxorubicin (Dox) is an effective anticancer drug used for the treatment of a number of carcinomas, such as breast, bladder, and gastric cancers.[28,29] Like most anticancer drugs, Dox can cause severe toxicity to the body such as myelosuppression, loss of hair, nausea, vomiting, mucositis and irreversible cardiac toxicity. [28,29]

Therefore, a site-specific and targeted DDS is essential to overcome these problems in the effective treatment of cancers using Dox as an anticancer agent. Application of liposomes,[30,31] hydrogels,[32] microspheres,[33] polymeric micelles,[34] drug-polymer conjugates,[35] magnetic nanoparticles [36,37] and nanofibrous scaffolds [38,39] have been reported in literature.

This study is the first attempt to produce a stimuli-responsive polymeric NFs from P(NIPAAm-AAm-VP) by water-based approaches without any further crosslinking step. Box–Benkhen design was used to investigate the effects of flow rate, solution concentration, voltage, and distance and optimization of parameters to obtain controllable diameter of these polymeric nanofibres. To investigate the utility of these biocompatible scaffolds as an implantable vehicle for long-term delivery of anticancer drugs, Dox-loaded NFs were prepared from these polymers via electrospinning method. *In vitro* release profile and antitumor activity of the Dox-containing fibers were also investigated. Scanning electron microscopy (SEM) images of the electrospun NFs revealed a continuous and smooth fibrous morphology. The stability of the NFs after immersion in phosphate buffered saline (PBS) (pH 7.4) at 37 °C (above the LCST of polymer) was studied by SEM observation.

2. Experimental procedures

2.1. *Materials*

N-isopropylacrylamide (NIPAAm) (Fluka) was purified by recrystallization in hexane and dried under vacuum at 25 °C. Vinyl pyrrolidone (VP) (Merck-Schuchardt Co.) was freed from stabilizer by twice vacuum distillation with continuous bubbling argon. Acrylamide (AAm) (Fluka) was purified by recrystallization in chloroform and dried under vacuum at 25 °C. Ammonium persulfate (APS) (Aldrich Chemical Co) was purified by recrystallization in EtOH/H_2O (2/1) solvent mixture and dried under vacuum at 40 °C and used as initiator. The accelerator N,N,N,N-tetramethyl ethylene diamine (TEMED) (Fluka) was used as supplied. Dox was purchased from Sobhan Pharmaceuticals, Iran.

2.2. *Polymer preparation*

Stimuli-responsive P(NIPAAm-AAm-VP) was prepared according to the method described previously.[40] Briefly, predetermined amounts of purified NIPAAm, AAm, and VP (molar feed ratio of NIPAAm to AAm to VP, 20:3:1) were dissolved in distilled water, into which 0.3 mol% APS with respect to all the monomers was added. The mixture was magnetically stirred and degassed with argon for 30 min. Then 30 mL of TEMED

was added as an accelerator. The polymerization was carried out at room temperature for 16 h with continuous argon bubbling. The obtained reaction mixture was purified by dialysis for 5 days using dialysis membrane (Cellu SepH1) with MWCO of 2000 and the external aqueous solution was removed two times a day and displaced with fresh distilled water. The polymer solutions were precipitated by heating them at temperatures above their LCST. The obtained gels were then dried in vacuum at 40 °C for 24 h and frozen in liquid nitrogen to be lyophilized immediately obtaining dry powder and dried again under vacuum at 40 °C for 24 h.

2.3. *Electrospinning*

P(NIPAAM-AAm-VP) was dissolved in distilled water and stirred for 24 h at 10 °C to produce a 10 wt.% solution. The electrospinning set-up has been described previously. [41] The well mixed P(NIPAAM-AAm-VP) solution was added in a 5 mL syringe with a right-angle shaped metal capillary attached to it. The circular orifice of the capillary has an inner diameter of 0.4 mm. The applied voltage was in the range of 15–25 kV. A pressure was applied to the solution in syringe to maintain a steady flow of the solution from the needle outlet in the range of 0.2–1 mL/h. The distance between the needle tip and the grounded target was adjusted in the range of 7–15 cm. All electrospinning experiments were carried out at about 20 °C in air. The electrospun fibrous scaffold was collected on a metal drum (9 cm diameter) as an electrode, rotating at approximately 1000 rpm. The resulting scaffold was vacuum dried at room temperature for a week to completely remove any solvent residue, prior to the experiments.

2.4. *Nanofiberous scaffold characterizations*

FTIR spectra of free and dox-loaded NFs were collected over the range of 4000–400 cm^{-1} by casting polymer solutions in CH_2Cl_2 on KBr windows using Bruker (Tensor 27) IR spectrophotometer instrument.

The crystalline states of Dox, P(NIPAAm-AAm-VP), and Dox-loaded P(NIPAAm-AAm-VP) fibers were analyzed by wide-angle X-ray diffraction (Siemens, D5000). The samples were scanned from 5° to 70° at a scanning rate of 5°/min.

The surface morphology of the electrospun nanofibrous scaffolds was examined with SEM (MV2300) after gold coating. From each image, at least 50 different fiber segments were randomly selected and their diameters were measured to generate an average fiber diameter. For samples with beads, both the NFs and beads were measured (fibers on the nanometer scale and beads on the micron scale). The average diameter and diameter distribution of NFs were obtained with an image analyzer (Image-Proplus, Media Cybrernetics).

UV–Vis (Shimatzo UV-1800 Series) measurement was carried out to demonstrate that the electrospinning process did not adversely affect the molecular structure of Dox.

2.5. *Design of electrospinning experiments and optimization by RSM*

RSM is essentially a particular set of mathematical and statistical methods for experimental design. BBD is a class of rotatable second-order designs based on three-level incomplete factorial designs where the variable combinations are at the midpoints of the edges of the variable space and at the center. An advantage of the BBD is that it does not contain combinations for which all factors are simultaneously at their highest or lowest levels. So these designs are useful in avoiding experiments performed under extreme conditions, for which unsatisfactory results are often obtained. The number of experiments (N) needed for the development of Box–Behnken experimental design is defined as $N = 2k(k-1) + C_0$, where (k) is the factor number and (C_0) is the replicate number of the central point.[42] In the current study, four-factor three-level BBD was used to determine the relation between variables containing the solution concentration (5–10 mg/L), applied voltage (15–25 kV), flow rate (0.2–1 mL/h), and target–collector distance (7–15 cm). The statistical calculation levels associated with each variable were summarized in Table 1. All experiments were repeated twice. The results of the experimental design were studied by MINITAB 16 (PA, USA) statistical software to estimate the response of the dependent variable.

The BBD response surface model of electrospinning experiments expresses the P(NIPAAM-AAm-VP) NFs diameter as a function of the above mentioned variables. The polynomial model for the NFs diameter with respect to the electrospinning variables is expressed as follows in Equation (1):

$$\text{Diameter of fiber} = \beta_0 + \sum_{i=1}^{3} \beta_i x_i^2 + \sum_{i=1}^{3} \beta_{ii} x_i^2 + \sum_{i=1}^{3} \times \sum_{j=1}^{3} \beta_{ij} x_{\{i\}} x_j \quad (1)$$

Table 1. Experimental ranges and levels of independent variables used in electrospinning process.

		Range of levels		
Variable	Code	−1	0	1
Concentration (mg/L)	$X1$	5	7.5	10
Voltage (kV)	$X2$	15	20	25
Flow rate (mL/hr)	$X3$	0.2	0.6	1.0
TCD (cm)	$X4$	7	11	15

where Y is the predict response by the model and β_0, β_i, β_{ii}, β_{ij} are the constant regression coefficient of the model X_i, X_{ii}, and X_{ij} represent the linear, quadratic and interactive terms of the uncoded independent variables, respectively. The coefficient of determination (R^2) was used to evaluate the accuracy of the full quadratic equation. The experimental design and results used for the study are shown in Table 2.

2.6. *Drug incorporation and encapsulation efficiency*

For the preparation of Dox-incorporated NFs, Dox was dissolved in polymer solution and stirred for 24 h at 10 °C. Dox was used at loading percentages of 10, 20, and 50% of the initial polymer weight. The homogeneous mixture of Dox and NFs was electrospun with optimum conditions of electrospinning process as described above.

To determine the encapsulation efficiency, 5 mg of Dox-loaded P(NIPAAm-AAm-VP) NFs were dissolved uniformly in 3 ml distilled water at 10 °C in the dark for 24 h. The drug content of the extracted solution was detected at 483 nm with an UV–Vis spectrophotometer, in which the concentration was obtained using a standard curve from known concentrations of Dox solutions.

Table 2. The experimental design and results.

Std. order	Voltage	Distance	Flow rate	Concentration	Result	Fitted value by model
1	15	7	0.6	7.5	206.901	201.623
2	25	7	0.6	7.5	229.229	197.981
3	15	15	0.6	7.5	249.234	232.693
4	25	15	0.6	7.5	199.458	204.295
5	20	11	0.2	5	241.091	220.852
6	20	11	1	5	224.790	231.173
7	20	11	0.2	10	247.893	216.374
8	20	11	1	10	261.372	226.696
9	15	11	0.6	5	237.239	220.807
10	25	11	0.6	5	235.234	204.788
11	15	11	0.6	10	246.125	216.330
12	25	11	0.6	10	235.235	200.311
13	20	7	0.2	7.5	239.239	198.690
14	20	15	0.2	7.5	270.025	235.714
15	20	7	1	7.5	262.067	227.344
16	20	15	1	7.5	239.239	227.703
17	15	11	0.2	7.5	258.229	220.610
18	25	11	0.2	7.5	248.298	204.591
19	15	11	1	7.5	267.243	230.932
20	25	11	1	7.5	245.243	214.913
21	20	7	0.6	5	215.215	208.053
22	20	15	0.6	5	223.642	226.745
23	20	7	0.6	10	263.262	203.576
24	20	15	0.6	10	257.543	222.268
25	20	11	0.6	7.5	179.553	179.072
26	20	11	0.6	7.5	180.023	179.072
27	20	11	0.6	7.5	178.987	179.072

2.7. In vitro *drug release behaviors of electrospun nonwoven fabrics*

The *in vitro* release profiles were investigated in phosphate buffer solution (pH 7.4). The amount of released Dox in the buffer solution was monitored by a UV–Vis spectrophotometer at the wavelength of 483.5 nm. Drug content was determined as a function of scaffold weight. The drug-loaded fiber sample (50 mg) was incubated at 37 °C in 20 mL of 0.1 M PBS (pH 7.4). The suspensions were kept in a thermostated shaking water bath (Hidolff) that was maintained at 37 °C and 100 rpm of stirring for 30 days. Samples of 2.0 mL released solution were taken from the dissolution medium at predetermined intervals, while equal amount of fresh buffer solutions was added back to the incubation media. The amount of Dox present in release buffer was determined by converting its detected UV absorbance to its concentration according to the calibration curve of known concentrations of Dox in the same buffer. A standard calibration plot of Dox with the concentrations from 5 to 500 ppm, linear correlations ($c2 = 0.9992$ in pH 7.4 buffer solution) was used to determine the concentration of the released drug. Then the percentage of the released Dox was calculated as a function of incubation time and based on the initial weight of the drug incorporated in the electrospun scaffold.

2.8. *Cell culture experiments*

Human lung carcinoma A549 cell line was obtained from National Cell Bank of Iran and maintained in 75 cm^2 culture flask, in Roswell Park Memorial Institute 1640 medium (RPMI 1640 medium; Gibco BRL Life Technologies) supplemented with 10% (v/v) fetal bovine serum and antibiotics (100 mg/ml penicillin–streptomycin). The cells were incubated at 37 °C in an atmosphere of 5% CO_2 and 95% air with more than 95% humidity; medium was changed every two days for cell feeding.

2.9. In vitro *cytotoxicity assay*

Cell viability was determined using a colorimetric 3-(4,5-Dimethylthiazol-2-yl)-2,5- diphenyltetrazolium bromide, a tetrazole (MTT) assay as previously described.[43] Briefly, the cells were cultured at 37 °C in a humidified atmosphere containing 5% CO_2, dissociated with 0.25% trypsin in PBS (pH 7.4) and centrifuged at 1000 rpm for 7 min at room temperature. Then 30,000 to 40,000 cells were cultured in each well of 96-well plates and after 24 h time periods, to allow attachment of the cell to the wells, different concentrations of the materials were treated to the cells. In this context, different concentrations (1, 0.8, 0.6, 0.4, and 0.2 mg/ml) of NFs, NF-Dox, and free Dox were prepared with 1% DMSO and treated to the cells at different time periods.

However, media containing 1% DMSO was used as negative control. The MTT assay was as follows: 20 µl of MTT solution (5 mg/ml) in PBS (pH 7.4) was added to each well. The incubation was continued for another 4 h and then the solution was aspirated cautiously from each well. After treating the cells with Sorenson buffer, the optical density of each well was read using a microplate reader (Multiskan MK3, Thermo Electron Corporation, USA) at a wavelength of 570 nm, and growth inhibition was calculated. All of the tests were performed in duplicate and statistical analyses were carried out using SPSS 15; $p < 0.05$ was considered significant.

3. Result and discussion

3.1. *Electrospinning process*

3.1.1. *Effect of electrospinning variables on NFs diameter*

The effect of the four experimental factors including solution concentration, applied voltage, flow rate, and tip–collector distance on the diameter of the electrospun P(NIPAAm-AAm-Vp) NFs was evaluated at the different experimental levels (Table 1 and Figure 1). Each figure indicates the effect of parameters at the center level of other parameters.

The polymer solution concentration was the most important parameter determining the fiber diameter. At low concentration, small fibers with beads were formed on the collector.[21,22] By increasing the concentration, the fibers showing smaller diameter and fewer beads were formed. The higher concentrations of spinning solution led to the formation of fibers with larger diameters.[23] The formation of beaded fibers in lower concentration is due to the stronger instabilities of jet solution under the electrical field. With increasing the concentration, the instabilities of jet solution decrease and fibers without any beads form on the collector.[24,25] At higher concentration, droplets form on the collector.[26] The effect of concentration on the diameter of fiber is shown in Figure 1(a). As can be seen from the figure, the fibers with larger diameters were formed, when the concentration of jet solution was 5%. Increase in the concentration to 7.5%, the conductivity and surface tension were also increased and thinner fibers were formed. At the concentration of 10%, the diameter of fibers was increased. The effect of flow rate on the diameter of electrospun fibers is shown in Figure 1(b). As can be seen, when the flow rate of spinning solution was increased to 0.6 ml/hr, the instability of solution jet due to the surface tension of fluid caused to verify the flow rate of solution. At the flow rate greater than 0.6 ml/hr, the diameter of fibers was increased. It could be due to decreasing of electrostatic density which caused to fabricate the fibers with greater diameters in higher flow rate. At flow rate lower than 0.2 ml/hr, the spinning solution was dried and the electrospinning process was stopped. The effect of voltage on the formation of electrospun fibers in the range of 15–25 kV is shown in Figure 1(c). At lower voltage, the electrical force was not enough to form the perfect fibers. When the voltage was 20 kV, uniform fibers with smallest diameter were obtained. When the applied voltage was greater than 20 kV, the strength of the electrical field was so high due to which the instabilities of jet solution increased and the fibers with larger diameter were formed on the collector. Figure 1(d) shows the effect of tip collector distance (TCD) on the diameter of electrospun fibers. As can be shown, at TCD of 7 cm, thicker fibers were formed on the collector. The fiber with smallest diameters was obtained, when the TCD was 11 cm. At TCD of 11 cm, the stability of jet increased resulting in the formation of thinner fibers. By increasing the TCD to 15 cm or higher than 15 cm, the strength of electrical force on the spinning solution decreased resulting in the formation of fiber with larger diameter.

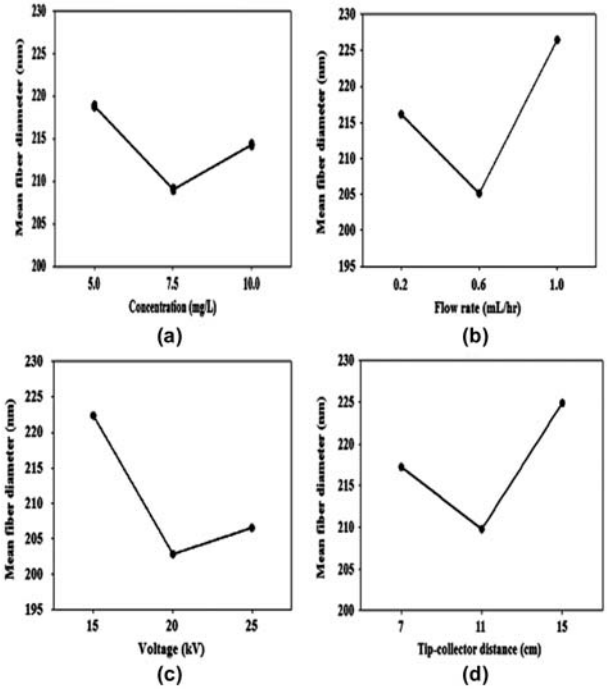

Figure 1. Effect of concentration, flow rate, voltage, and distance on the diameter of electrospun fibers.

3.1.2. *Analysis of experimental design*

Four factors of electrospinning process including concentration, voltage, flow rate, and TCD at three levels for fabrication of uniform P(NIPAAM-AAm-VP) fibers were performed. ANOVA was performed to evaluate a full quadratic response surface model. *P*-value is a measure of statistical significance and the electrospinning parameter shows significant impact on the average fiber

Table 3. ANOVA results for experimental response at different factor levels.

Source	DF	*F*	*P*
Regression	14	9.23	0.000
Linear	4	6.73	0.004
Voltage	1	7.91	0.016
Distance	1	5.92	0.032
Flow rate	1	8.27	0.014
Concentration	1	22.18	0.001
Square	4	19.34	0.000
Voltage × voltage	1	15.05	0.002
Distance × distance	1	27.88	0.000
Flow rate × flow rate	1	62.46	0.000
Concentration × concentration	1	32.60	0.000
Interaction	6	2.28	0.106
Voltage × distance	1	2.66	0.129
Voltage × flow rate	1	0.08	0.785
Voltage × concentration	1	0.39	0.546
Distance × flow rate	1	5.84	0.032
Distance × concentration	1	2.47	0.142
Flow rate × concentration	1	2.21	0.163
Residual error	12	690.09	57.51
Lack-of-fit	10	30.77	0.032
Pure error	2	4.46	2.23
Total	26	8121.32	

diameter while the *P*-value is less than 0.05 at 95% confidence interval. The ANOVA results (Table 3) of the experimental data reveal that the model is statistically significant with linear, quadratic, and flow rate-distance interaction terms ($p \leqslant 0.05$). Other interaction terms were statically insignificant ($p > 0.05$).

By elimination of insignificant terms ($p > 0.05$) from the full quadratic model (Table 4), the Equation (2) which including a series of significant terms for the four electrospinning variables is designed as follows as:

$$\begin{aligned}\text{Diameter of fiber (nm)} = {} & 708.634 - 21.982x_1 \\ & - 18.067x_2 - 118.721x_3 \\ & - 45.895x_4 + 0.509x_1^2 \\ & + 1.089x_2^2 + 162.201x_3^2 \\ & + 3.0x_4^2 - 5.729x_2x_3 \qquad (2)\end{aligned}$$

Table 4. Regression coefficients for the response surface model.

Term	Coef	*T*	*P*
Constant	708.634	7.851	0.000
Voltage	−21.982	−3.862	0.001
Distance	−18.067	−3.512	0.003
Flow rate	−118.721	−3.031	0.008
Concentration	−45.895	−5.361	0.000
Voltage × voltage	0.509	3.593	0.002
Distance × distance	1.084	4.891	0.000
Flow rate × flow rate	162.201	7.320	0.000
Concentration × concentration	3.000	5.289	0.000
Distance × flow rate	−5.729	−2.239	0.039

The goodness-of-fit measure of the model was evaluated using the coefficient of determination (R^2). The R^2 obtained was 0.9532, which indicated that 95.32% of the total variations could be explained by the model. The high value of R^2 ($R^2 = 0.9533$) indicated a high reliability of the model in predicting the average diameter of P (NIPAAM-AAm-VP) NFs.

3.1.3. *Counter plots analysis*

In order to gain a better understanding of the influences of the variables and their interactions on the diameters of P(NIPAAM-AAm-VP), counter plots for the measured responses (nm) were formed based on the model equation. Figure 2 shows counter plots of the response variable (Mean fiber diameter) for the experimental factors (two factor at-a-time). Each figure indicates the relation between the two parameters at the center level of third and forth parameters on the fiber diameter (nm).

The counter plot for the concentration vs. flow rate (Figure 2(a)) showed that the certain value for concentration with varying the flow rate was led to produce the fibers with smaller diameters.

Figure 2(b) shows that the lower or/and higher distances with combining the lower or/and higher concentration were not suitable for fabrication of homogeneous

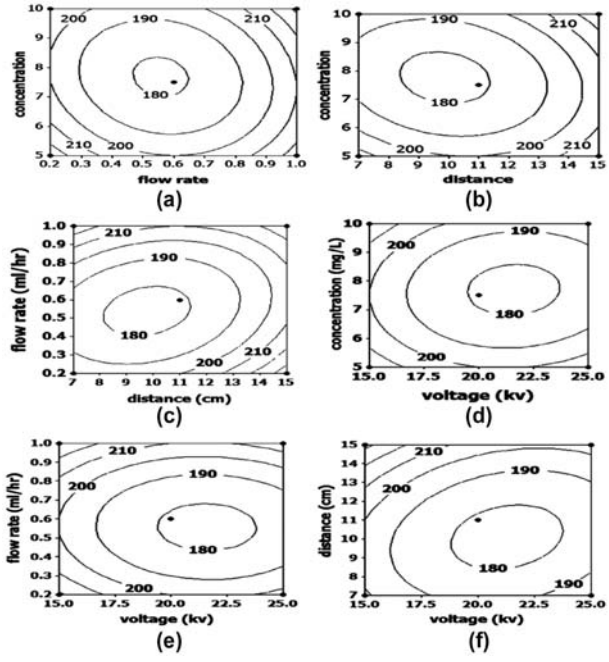

Figure 2. Counter plots of the response variable (fiber diameter (nm)) for the different experimental factors (two-factor-at-a-time). (a) Flow rate and polymer solution concentration, (b) distance and polymer solution concentration, (c) flow rate and distance, (d) polymer solution concentration and applied voltage, (e) flow rate and applied voltage, and (f) distance and applied voltage.

and thin fibers. Figure 2(c) shows that the variation in the flow rate and distance values produced fibers of smaller diameters. Figure 2(d) and (e) shows that the diameter reduction of fibers was controlled with higher voltage values in comparison to lower voltage values. Also, Figure 2(f), on the other hand, shows that the combination of high voltage values with varying distances favored the formation of fibers with smaller diameters.

3.1.4. *Optimization of the electrospun fiber diameter*

By solving the Equation (2), the optimal uncoded values of concentration ($X1$), flow rate ($X2$), distance ($X3$), and voltage ($X4$) were estimated to be 7.65 mg/L, 0.54 mL/h, 9.75 cm, and 21.57 kV, respectively, which in turn yielded a minimum fiber diameter of 175.90 nm. For electrospinning parameters, the experimental NFs diameter (176.57 nm) was 0.4% further than the value predicted by the model (175.90 nm) which is ignorable since the results were too closer to each other. The SEM graphs of fiber scaffolds before (a) and after (b) optimization of electrospinning process are shown in Figure 3. As can be seen, by optimizing the parameters, the thinner fibers with sharp diameter distribution in comparison to thinnest fibers before optimization were formed.

3.1.5. *Model verification with experimental data*

Figure 4(a) shows the experimental fiber diameter against the model predicted fiber diameter and the linear correlation coefficient was evaluated. The linear adjusted correlation coefficient of 0.912 was obtained. The value of adjusted correlation coefficient indicated a reasonable relationship between the experimental data and model values. The probability distribution plot of residuals (difference between the model predicted fiber diameter values and those derived experimentally) is presented in Figure 4(b). As can be seen, the errors were normally distributed, as all the points were close to the line.

3.2. *Morphology of electrospun Dox-loaded nanofibrous scaffolds*

The SEM micrograph of the electrospun Dox-loaded P (NIPAAm-AAm-VP) NFs with 10, 20, and 50 wt.% of Dox loadings is shown in Figure 5(a, b and c). It seems the samples were uniform. The surfaces were smooth and no drug crystals were identified, indicating that the drug was finely incorporated into the electrospun fibers. The color of the fibers became much more even and no Dox crystals could be found on the fiber surface. Furthermore, the average diameter of the NFs was increased by the increasing amounts of Dox. The average diameter of 10, 20, and 50 wt.% of Dox-loaded P(NIPAAm-AAm-VP) NFs was obtained about 346.76, 368.83, and 384.41 nm. Dox is a hydrophilic drug and was highly soluble in the polymer solution.

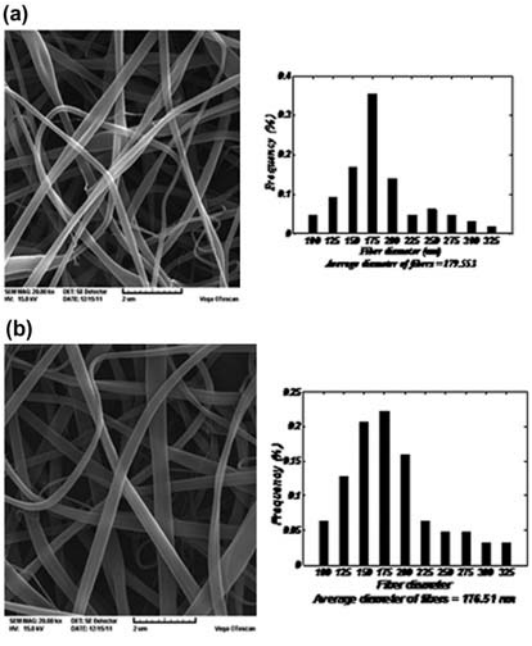

Figure 3. The SEM graphs of fiber scaffolds before (a) and after (b) optimization of electrospinning process.

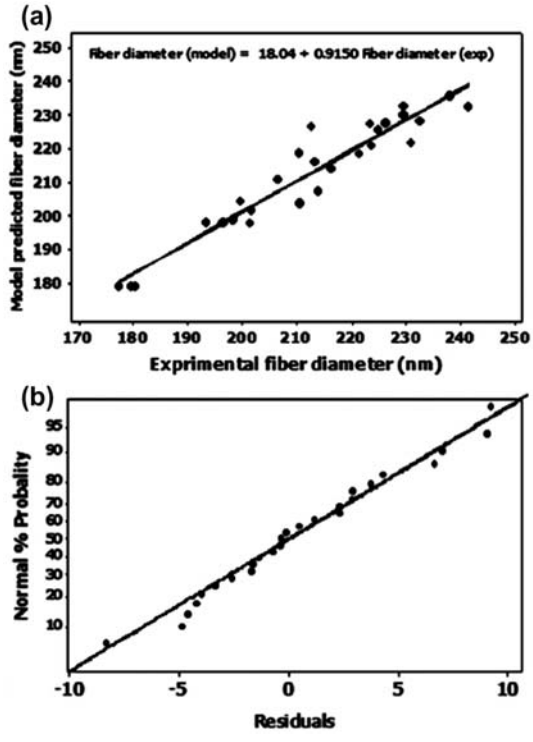

Figure 4. (a) Plot of model predicted fiber diameter against experimental fiber diameter, (b) normal probability plot.

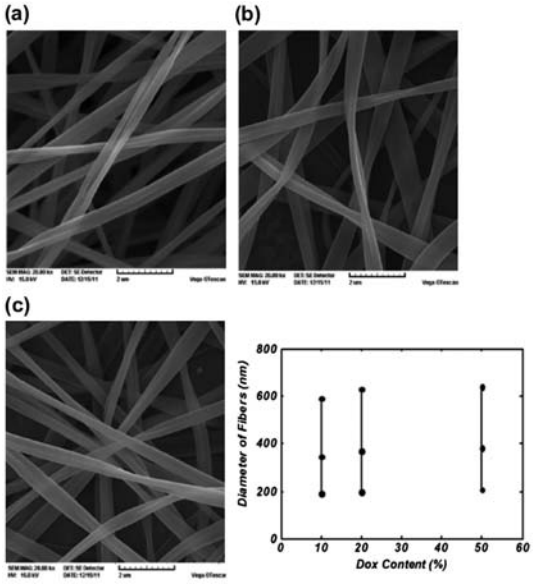

Figure 5. The SEM micrograph of the distribution of the electrospun Dox-loaded P(NIPAAm-AAm-VP) NFs with 50 (a), 20 (b), and 10 (c) wt.% of Dox.

3.3. *Characterization of Dox-loaded NFs*

UV–Vis measurement was carried out to demonstrate that the electrospinning process did not adversely affect the molecular structure of Dox.[44] Figure 6 shows the spectroscopic characterizations of the released Dox using UV–vis measurements. The spectra of pure and released Dox (at different release time) from A_1 formulation show similar maximum absorbance peak at 483 nm.

The FTIR spectra of P(NIPAAM-AAm-VP) NFs(a) and Dox-loaded P(NIPAAM-AAm-VP) NFs (b) were shown in Figure 7. Characteristic peaks of doxorubicin at 1750 related to carbonyl groups of cyclohexanone ring

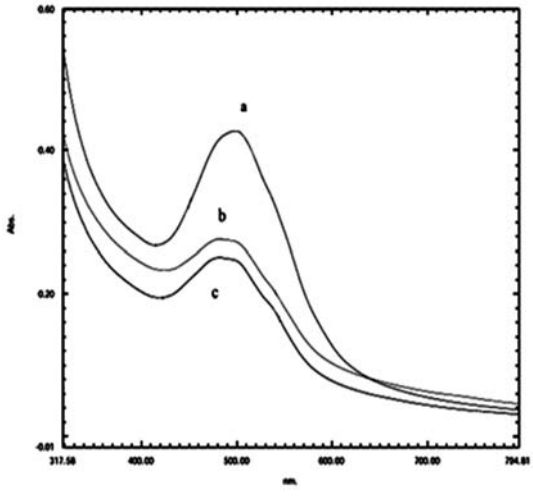

Figure 6. UV–Vis spectra of pure doxorubicin (a) and released doxorubicin from A_1 electrospun scaffolds after one week (b) after two weeks (c).

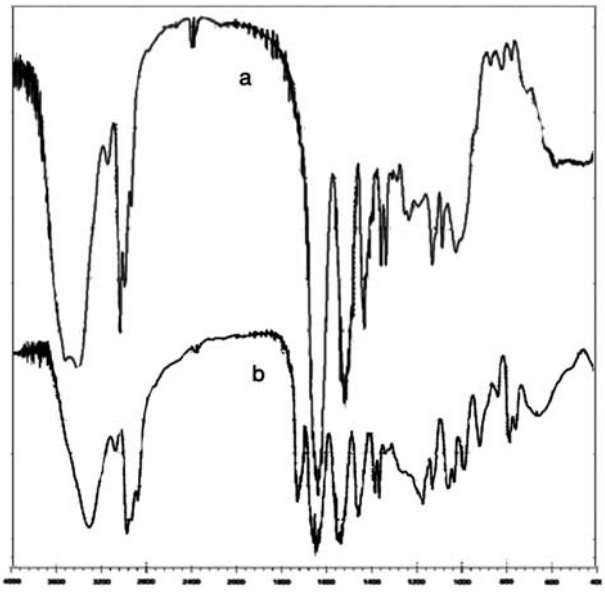

Figure 7. The FTIR spectra of P(NIPAAM-AAm-VP) NFs (a) and Dox-loaded P(NIPAAM-AAm-VP) NFs (b).

of doxorubicin. The peaks at 1650 and 1550 cm^{-1} were assigned to amide I (C=O stretching) and amide II (N–H bending) of the copolymer, respectively. The broad absorption band observed around 3430 cm^{-1} was assigned to the N–H stretching of amide groups in the copolymer. The peaks at 1370–1390 and 2980 cm^{-1} were assigned to the stretching modes of the $–CH(CH_3)_2$ and $–(CH_3)_2$ groups in NIPAAm, respectively. Other characteristic peaks of Dox overlapped with polymer.

To further demonstrate the physical state of Dox in the fibers, Dox, P(NIPAAM-AAm-VP), and Dox-loaded P(NIPAAM-AAm-VP) fiber mats were characterized by XRD.[45–47] As shown in Figure 8, pure Dox is crystalline, with many characteristic peaks, while P(NIPAAM-AAm-VP) fibers are amorphous. The crystalline Dox is not detected in all Dox-containing P(NIPAAM-AAm-VP) fibers, suggesting that Dox exists in amorphous form, probably as a solid solution or amorphous molecular aggregates in P(NIPAAM-AAm-VP) fibers.

3.4. *Encapsulation efficiency and in vitro release*

In order to ensure effective encapsulation of the drug inside the polymeric fibers and thus to achieve a constant and stable drug release profile, a lipophilic polymer should be chosen as the fiber material for a lipophilic drug ,while a hydrophilic polymer should be used for a hydrophilic drug and the solvents used should be good for both the drug and the polymer(compatible drug with polymers).The burst release of the drugs can be avoided by using these systems, and the drug release can follow nearly zero-order kinetics.[13] For example, nearly zero-

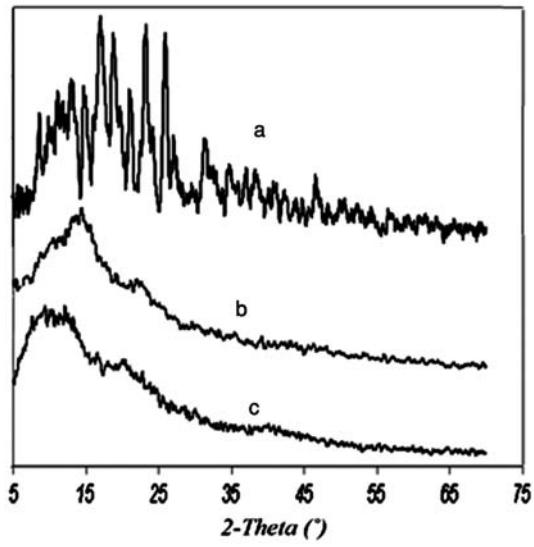

Figure 8. XRD patterns of Dox powders (A), P(NIPAAm-AAm-VP) NFs (B) and 50% Dox-loaded P(NIPAAm-AAm-VP) NFs (C).

order kinetics was observed for Dox release from PLLA NFs in the presence of protinease K during 7 h.[14]

In this study a compatible drug with polymer system has been used for preparation of Dox-loaded NFs. Figure 9 shows the release profiles of Dox from 50, 20, and 10 wt.% Dox-loaded fibers (A_1, A_2, and A_3) respectively up to 30 days. An approximately linear relationship between the drug release (%) and time is seen. The drug release behaviors were similar for three different formulations, that is, after a small burst release at first 30 min, the release rate of Dox leveled off. For example, their release percentages were about 9.1, 6.9, and 3.5% after 30 min and about 82.1, 65.17, and 53.9% (A_3, A_2, and A_1) respectively after 30 days, for the three samples examined. *In vitro* drug release study indicated that prepared polymeric implants provided zero-order release kinetics of drug ($R^2 > 0.98$ for all equations obtained from data plotting the percent of drug released vs. time). The potential for drug delivery at a rate which is independent of time and the concentration of drug within a pharmaceutical dosage form is desirable. Zero-order mechanism ensures that a steady amount of drug is released over time, minimizing potential peak/trough fluctuations and side effects, while maximizing the amount of time the drug concentrations remain within the therapeutic window (efficacy). The statistical comparison among slop of release equations showed no significant differences (p-value > 0.05), which indicates that the drug release rate is not dependent on drug/polymer ratio in different implant formulations. This finding can be claimed as one of the advantages of the developed delivery system. Initial burst release of Dox-fibers within 30 min was mainly due to the diffusion of Dox dispersing close to the surface of polymer fibers, which diffused out quickly in initial incubation time. The pores left after initial burst release and subsequent drug diffusion were critical for further release from the inner sections of fibers through the swollen and porous inner structure. This was caused by the relative hydrophilic surface, which assisted water diffusion in and drug diffusion out of the fiber matrix. The porous structure of fibrous mats and the micropores after the diffusion of drug from the polymers made it possible for further constant release of drug from inner matrix. In all three samples, relatively small burst release was initially observed followed by a steady or gradual release during the rest time. The initial amount of the released drug was found to vary as a function of drug concentration. Obviously, in the whole drug release period, the release rate of Dox decreased with increasing Dox content. Thus, it may be concluded that relatively small burst release and higher sustained release rate can be achieved from all three formulation. During electrospinning, if there are limited physical interactions between the drug and the polymer matrix, then most of the drug will be located on the surface of the NFs due to the high ionic strength of the drug. In such an arrangement, the drug molecules on the fiber surface can be easily washed away in aqueous solutions, thus resulting in a large initial burst at short times and minimum sustained release at longer times. Figure 9 showed small amount of initial burst release and sustain release of drug for more than 30 days. It means that most of the drug was incorporated inside the NFs. For the delivery of anticancer drugs, a certain amount of initial burst is actually required to achieve enough initial dosage. Of course, for the cancer cells that survive the initial stage, sustained drug release is necessary. Therefore it is interesting to note that the Dox-loaded P(NIPAAm-AAm-Vp) (molar

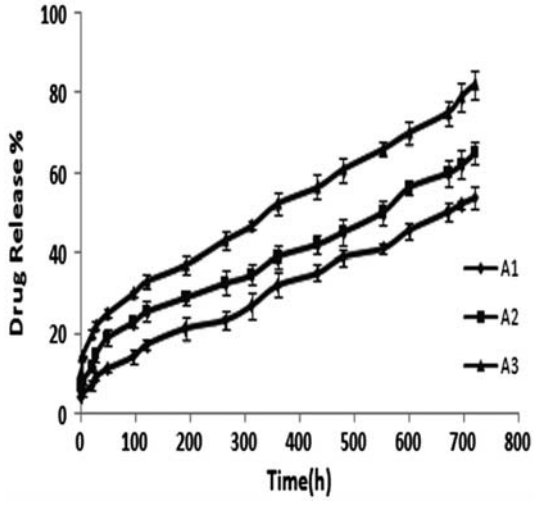

Figure 9. Release profiles of Dox from 50, 20, and 10 wt.% Dox-loaded fibers (A_1, A_2, and A_3).

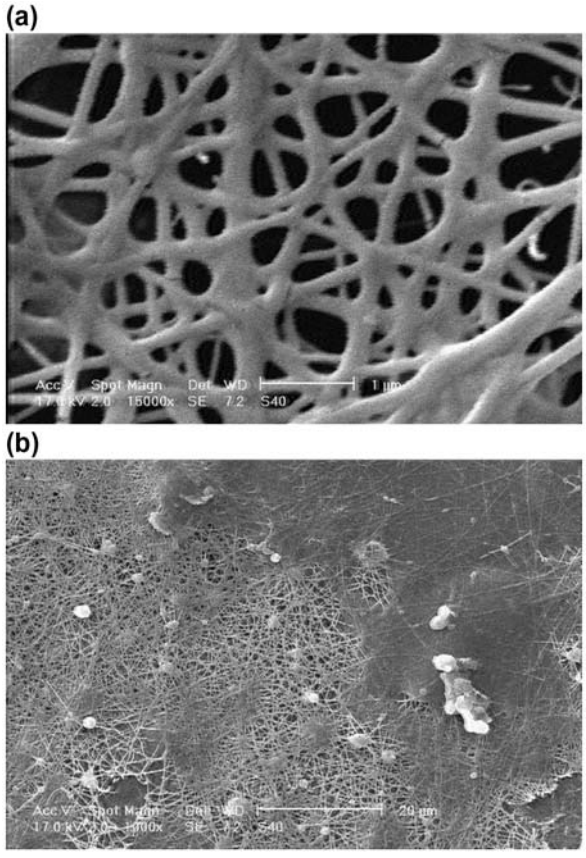

Figure 10. SEM image of the Dox-loaded P(NIPAAm-AAm-VP) NFs after 14 (a) and 21 (b) days of incubation in release medium (pH 7.4, 37 °C).

ratio of 20:0.5:4) nanofibrous scaffold showed a sustained release profile after the initial burst and exhibit an ideal release profile for potential cancer therapy.

The stability of the P(NIPAAm-AAm-Vp) NFs after immersion in PBS (pH 7.4) at 37 °C (above the LCST of polymer) was studied by SEM observation (Figure 10). As shown in Figure 10 NFs maintain its structure during release period but because of the sol-gel properties of these thermosensitive NFs, three-dimensional structure was formed above the LCST of polymer (Figure 10). The slow drug release pattern can be interpreted by the formation of such a three-dimensional fibrous structure. If the NFs maintained its linear structure or degraded, the rapid release of drug was possible to be observed. Figure 9 indicates that the drug release profile is constant and shows nearly zero-order kinetics during 30 days of incubation in pH 7.4, 37 °C. It seems that the dissolution of NFs is very slow till 30 days that could not affect the zero-order kinetics of drug release.

This very slow water solubility in physiological condition would give P(NIPAAm-AAm-VP) NFs good potential for DDSs or implant applications. Therefore, these NFs will be used as stimuli-sensitive drug carriers in a new DDS based on the use of thermosensitive polymers.

3.5. *Cytotoxicity tests*

Figure 11 shows the cell growth inhibition after 72 h incubation for the free Dox, the Dox-loaded fibers, and the pure P(NIPAAM-AAm-VP) fibers without drug. Paired sample student's *t*-test revealed that at the same treatment dose Dox-loaded P(NIPAAM-AAm-VP) fibers exhibited more antitumor activity compared with free Dox. (data not shown; $p > 0.05$) (Figure 12). It implied that the Dox-loaded P(NIPAAM-AAm-VP) fibers exhibited obvious cytotoxicity against A549 cells for more longer time than free Dox due to its capacity of sustained released time. Moreover, the Dox was released from P(NIPAAM-AAm-VP) fibers without losing cytotoxicity during a long time period (48–72 h) which seems to be more potent than free Dox with 16–18 h half life. [48] The cytotoxicities of the Dox-loaded P(NIPAAM-AAm-VP) fiber mats are shown in Figure 13. In the case of blank fiber mats without Dox, the sample did not display any cytotoxicity to A549 cells compared with the control up to 72 h (Figures 11 and 13). However, 72 h treatment of the cells with 0.2 to 1 mg/ml of Dox-loaded P(NIPAAM-AAm-VP) fiber mats cause nearly 65–91% cells death, respectively, which is very high compared with free Dox (60–62%), yet the free NFs showed nontoxic properties and the growth rate of synthetic mats treated cells is same as nontreating savage cells (Figures 11 and 12). These finding shows that Dox-loaded P(NIPAAM-AAm-VP) fiber mats can be used as an alternative source of free Dox due to its continuous release capacity over a long time from the P(NIPAAM-AAm-VP) fiber mats without losing its anticancer capability and, finally, fewer side effects.

4. Conclusion

In this study, P(NIPAAm-AAm-Vp) nanofibrous scaffold was fabricated for the first time by clean and safe electrospinning without using any toxic solvent or crosslinking agent. Dox, an anticancer drug, was successfully encapsulated into these nanofibrous scaffolds. The fibers had smooth and uniform surfaces. Dox was finely incorporated in the fibers and no Dox crystals were detected on the fiber surfaces. The release rate of Dox from the fibers was dependent on the initial Dox loading. During the whole release time, the rate of Dox release decreased as the Dox content in the fibers increased. Drug release pattern from these systems is in zero-order and drug release rate is not dependent on drug/polymer ratio in different implant formulations. The sustained release could last for more than 30 days. NFs were insoluble and could maintain its morphology during immersion in PBS at 37 °C. Cell toxicity

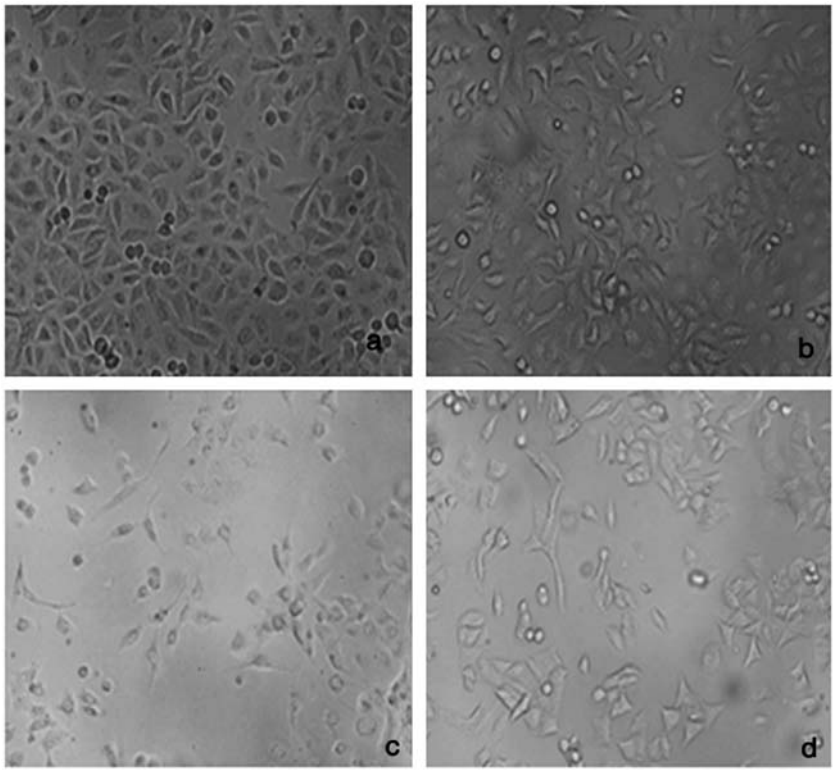

Figure 11. (a) Native human lung epithelial carcinoma A549 cell lines, treated by (b) Free NFs, (c) Nanodox and (d) Dox.

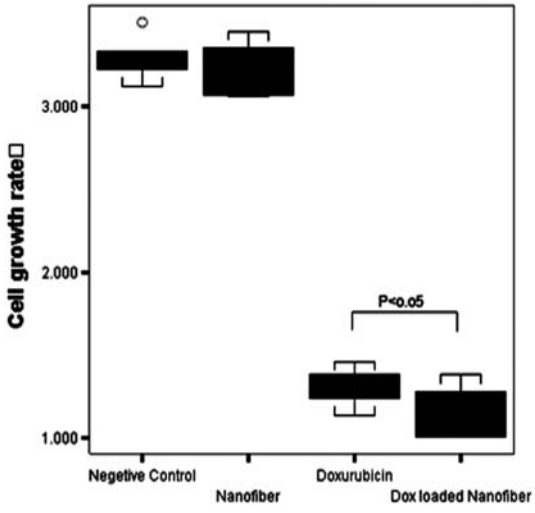

Figure 12. The Box-plot graph of cell growth rate by 1000 μg/ml treatment of NFs, Dox, and Dox-loaded NFs after 72 h incubation. RPMI 1640 containing 1% DMSO used as negative treatment control.

assays results revealed that cytotoxic activity of the Dox released from nontoxic P(NIPAAm-AAm-Vp) fibers was kept during the whole test for 72 h, while cytotoxic activity of pristine Dox was lost due to its short half-life.

Therefore, this sustained release delivery of Dox from P(NIPAAm-AAm-Vp) electrospun NFs has made it as long-term implantable drug delivery device for the treatment of lung cancer.

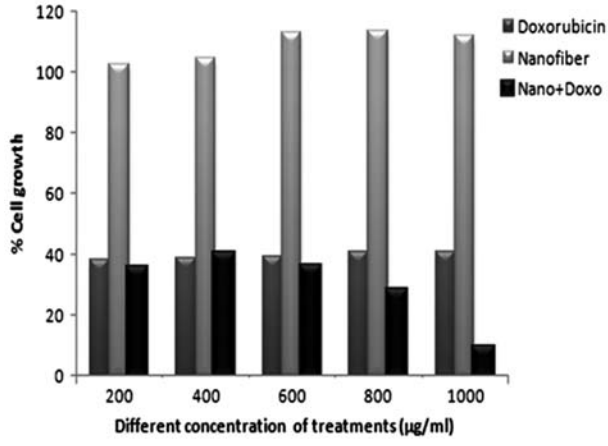

Figure 13. Cell growth inhibition rates by different concentration of Dox, free NFs, and Dox-loaded NFs.

References

[1] Langer R. Drug delivery and targeting. Nature. 1998;392:5–10.
[2] Brouwers JR. Advanced and controlled drug delivery systems in clinical disease management. Pharm. World Sci. 1996;18:153–162.

[3] Ahmed N, Fessi H, Elaissari A. Theranostic applications of nanoparticles in cancer. Drug Discovery Today. 2012. doi:10.1016/j.drudis.2012.03.010
[4] Vandghanooni S, Eskandani M. Comet assay: a method to evaluate genotoxicity of nano-drug delivery system. BioImpacts. 2011;1:87–97.
[5] Liu H, Hsieh YL. Ultrafine fibrous cellulose membranes from electrospinning of cellulose acetate. J. Polym. Sci., Part B: Polym. Phys. 2002;40:2119–2129.
[6] Zhang Y, Ouyang H, Lim CT, Ramakrishna S, Huang ZM. Electrospinning of gelatin fibers and gelatin/PCL composite fibrous scaffolds. J. Biomed. Mater. Res. B: Appl. Biomater. 2005;72:156–165.
[7] Kim HW, Song JH, Kim HE. Nanofiber generation of gelatin-hydroxyapatite biomimetics for guided tissue regeneration. Adv. Funct. Mater. 2005;15:1988–1994.
[8] Verpoest I, Lomov SV. Virtual textile composites software: integration with micro-mechanical, permeability and structural analysis. Compos. Sci. Technol. 2005;65:2563–2574.
[9] Qi M, Li X, Yang Y, Zhou S. Electrospun fibers of acid-labile biodegradable polymers containing ortho ester groups for controlled release of paracetamol. Eur. J. Pharm. Biopharm. 2008;70:445–452.
[10] Xie J, Wang CH. Electrospun micro- and nanofibers for sustained delivery of paclitaxel to treat C6 glioma *in vitro*. Pharm. Res. 2006;23:1817–1826.
[11] Wang Y, Wang B, Qiao W, Yin T. A novel controlled release drug delivery system for multiple drugs based on electrospun nanofibers containing nanoparticles. J. Pharm. Sci. 2010;99:4805–4811.
[12] Katti DS, Robinson KW, Ko FK, Laurencin CT. Bioresorbable nanofiber-based systems for wound healing and drug delivery: optimization of fabrication parameters. J. Biomed. Mater. Res. B Appl. Biomater. 2004;70:286–296.
[13] Zeng J, Yang L, Liang Q, Zhang X, Guan H, Xu X, Chen X, Jing X. Influence of the drug compatibility with polymer solution on the release kinetics of electrospun fiber formulation. J. Controlled Release. 2005;105:43–51.
[14] Zeng J, Xu X, Chen X, Liang Q, Bian X, Yang L, Jing X. Biodegradable electrospun fibers for drug delivery. J. Controlled Release. 2003;92:227–231.
[15] Chuang WJ, Chiu WY. Thermo-responsive nanofibers prepared from poly(*N*-isopropylacrylamide-co-*N*-methylol acrylamide). Polymer. 2012;53:2829–2838.
[16] Cui W, Qi M, Li X, Huang S, Zhou S, Weng J. Electrospun fibers of acid-labile biodegradable polymers with acetal groups as potential drug carriers. Int. J. Pharm. 2008;361:47–55.
[17] Kim YJ, Ebara M, Aoyagi T. Temperature-responsive electrospun nanofibers for 'on–off' switchable release of dextran. Sci. Technol. Adv. Mater. 2012;13:1–9.
[18] Bhattarai N, Zhang M. Controlled synthesis and structural stability of alginatebased nanofibers. Nanotechnology. 2007;18:455601–455609.
[19] Zhang Y, Su B, Venugopal J, Ramakrishna S, Lim C. Biomimetic and bioactive nanofibrous scaffolds from electrospun composite nanofibers. Int. J. Nanomed. 2007;2:623–638.
[20] Sun Z, Zussman E, Yarin AL, Wendorff JH, Greiner A. Compound core–shell polymer nanofibers by co-electrospinning. Adv. Mater. 2003;15:1929–1932.
[21] Liang D, Hsiao BS, Chu B. Functional electrospun nanofibrous scaffolds for biomedical applications. Adv. Drug Deliv. Rev. 2007;59:1392–1412.
[22] Theron S, Zussman E, Yarin A. Experimental investigation of the governing parameters in the electrospinning of polymer solutions. Polymer. 2004;45:2017–2030.
[23] Sajeev U, Anoop Anand K, Menon D, Nair S. Control of nanostructures in PVA, PVA/chitosan blends and PCL through electrospinning. Bull. Mater. Sci. 2008;31: 343–351.
[24] Heikkilä P, Harlin A. Parameter study of electrospinning of polyamide-6. Eur. Polymer J. 2008;44:3067–3079.
[25] Myers RH, Montgomery DC, Anderson-Cook CM. Response surface methodology: process and product optimization using designed experiments. New York (NY): Wiley; 2009.
[26] Box GEP, Draper NR. Empirical model-building and response surfaces. New York (NY): John Wiley & Sons; 1987.
[27] Sharma P, Singh L, Dilbaghi N. Optimization of process variables for decolorization of Disperse Yellow 211 by *Bacillus subtilis* using Box–Behnken design. J. Hazard. Mater. 2009;164:1024–1029.
[28] Tian Y, Bromberg L, Lin S. Complexation and release of doxorubicin from its complexes with pluronic P85-*b*-poly (acrylic acid) block copolymers. J. Controlled Release. 2007;121:137–145.
[29] Liu Z, Cheung R, Wu XY, Ballinger JR, Bendayan R, Rauth AM. A study of doxorubicin loading onto and release from sulfopropyl dextran ion-exchange microspheres. J. Controlled Release. 2001;77:213–224.
[30] Gabizon A, Martin F. Polyethylene glycol-coated (pegylated) liposomal doxorubicin. Rationale for use in solid tumours. Drugs. 1997;54:15–21.
[31] Wang S, Xu H, Xu J, Zhang Y, Liu Y, Deng YH, Chen D. Sustained liver targeting and improved antiproliferative effect of doxorubicin liposomes modified with galactosylated lipid and PEG-lipid. AAPS PharmSciTech. 2010;11: 870–877.
[32] Ta HT, Dass CR, Larson I, Choong PFM, Dunstan DE. A chitosan–dipotassium orthophosphate hydrogel for the delivery of doxorubicin in the treatment of osteosarcoma. Biomaterials. 2009;30:3605–3613.
[33] Dai Y, Ma P, Cheng Z, Kang X, Zhang X, Hou Z, Li C, Yang D, Zhai X, Lin J. Up-conversion cell imaging and pH-induced thermally controlled drug release from NaYF4: Yb3+/Er3+@hydrogel core–shell hybrid microspheres. ACS Nano. 2012;6:3327–3338.
[34] Yang SR, Lee HJ, Kim JD. Histidine-conjugated poly (amino acid) derivatives for the novel endosomolytic delivery carrier of doxorubicin. J. Controlled Release. 2006;114:60–68.
[35] Rıhová B, Etrych T, Pechar M, Jelı´nková M, Šťastný M, Hovorka O, Kovar M, Ulbrich K. Doxorubicin bound to a HPMA copolymer carrier through hydrazone bond is effective also in a cancer cell line with a limited content of lysosomes. J. Controlled Release. 2001;74:225–232.
[36] Akbarzadeh A, Mikaeili H, Zarghami N, Mohammad R, Barkhordari A, Davaran S. Preparation and *in vitro* evaluation of doxorubicin-loaded Fe_3O_4 magnetic nanoparticles modified with biocompatible copolymers. Int. J. Nanomed. 2012;7:511–526.
[37] Akbarzadeh A, Zarghami N, Mikaeili H, Asgari D, Goganian AM, Khiabani HK, Samiei M, Davaran S. Synthesis, characterization, and *in vitro* evaluation of novel polymer-coated magnetic nanoparticles for controlled delivery of doxorubicin. Nanotechnol. Sci. Appl. 2012;5:13–25.

[38] Zeng J, Yang L, Liang Q, Zhang X, Guan H, Xu X, Chen X, Jing X. Influence of the drug compatibility with polymer solution on the release kinetics of electrospun fiber formulation. J. Controlled Release. 2005;105:43–51.

[39] Xu X, Chen X, Ma P, Wang X, Jing X. The release behavior of doxorubicin hydrochloride from medicated fibers prepared by emulsion-electrospinning. Eur. J. Pharm. Biopharm. 2008;70:165–170.

[40] Salehi R, Arsalani N, Davaran S, Entezami A. Synthesis and characterization of thermosensitive and pH-sensitive poly(N-isopropylacrylamide-acrylamide-vinylpyrrolidone) for use in controlled release of naltrexone. J. Biomed. Mater. Res., Part A. 2009;89:919–928.

[41] Zong X, Kim K, Fang D, Ran S, Hsiao BS, Chu B. Structure and process relationship of electrospun bioabsorbable nanofiber membranes. Polymer. 2002;43:4403–4412.

[42] Ferreira SLC, Bruns R, Ferreira H, Matos G, David J, Brandao G, da Silva EG, Portugal LA, dos Reis PS, Souza AS, dos Santos WN. Box–Behnken design: an alternative for the optimization of analytical methods. Anal. Chim. Acta. 2007;597:179–186.

[43] Xu X, Yang L, Xu X, Wang X, Chen X, Liang Q, Zeng J, Jing X. Ultrafine medicated fibers electrospun from W/O emulsions. J. Controlled Release. 2005;108:33–42.

[44] Kim K, Luu YK, Chang C, Fang D, Hsiao BS, Chu B, Hadjiargyrou M. Incorporation and controlled release of a hydrophilic antibiotic using poly(lactide-co-glycolide)-based electrospun nanofibrous scaffolds. J. Controlled Release. 2004;98:47–56.

[45] Xu X, Chen X, Lu T, Wang X, Yang L, Jing X. BCNU-loaded PEG–PLLA ultrafine fibers and their *in vitro* antitumor activity against glioma C6 cells. J. Controlled Release. 2006;114:307–316.

[46] Cui W, Qi M, Li X, Huang S, Zhou S, Weng J. Electrospun fibers of acid-labile biodegradable polymers with acetal groups as potential drug carriers. Int. J. Pharm. 2008;361:47–55.

[47] Bhattarai N, Cha DI, Bhattarai SR, Khil MS, Kim HY. Biodegradable electrospun mat: novel block copolymer of poly(p-dioxanone-co-L-lactide)-block-poly(ethylene glycol). J. Polym. Sci., Part B: Polym. Phys. 2003;41:1955–1964.

[48] Laginha KM, Verwoert S, Charrois GJ, Allen TM. Determination of doxorubicin levels in whole tumor and tumor nuclei in murine breast cancer tumors. Clin. Cancer Res. 2005;11:6944–6949.